Quantum Control of Nuclear Motion at a Metal Surface†

H. Petek,* H. Nagano, M. J. Weida, and S. Ogawa

Advanced Research Laboratory, Hitachi, Ltd., Hatoyama, Saitama 350-0395, Japan

Received: March 30, 2000

The possibility of quantum control of surface photochemical reactions is demonstrated for the system of Cs/Cu(111). Coherent nuclear wave packet motion is induced by resonant dipole excitation with 3.08 eV light from an occupied surface state intrinsic to the Cu(111) surface to an unoccupied Cs antibonding state for a Cs atom coverage of 0.1 monolayer. Interferometric time-resolved two-photon photoemission measurements show that the polarization induced between the two states decays in ~25 fs. This makes it possible to control the position and momentum of the excited state wave packet through the phase of the excitation field. Quantum control is demonstrated for excitation with phase-related <20 fs pulse pairs or single chirped laser pulses. The phase dependence of two-photon photoemission spectra demonstrates the control of desorptive motion of Cs atoms.

I. Introduction

A longstanding goal in the field of chemistry, and a central theme of research in the Moore group, is the laser activation of nonthermal, bond-specific chemical reactions. The advent of lasers brought promise of relatively cheap and bright monochromatic radiation that could potentially induce selective chemistry otherwise not possible by conventional means. Much research has focused on activation and reaction of specific bonds through vibrational excitation.[1,2] A more recent approach is to perform specific chemical transformations by actively manipulating the quantum mechanical properties of molecules with light.[3,4] The major hurdle to achieving practical laser control of chemical reactions is the transfer of energy among the various nuclear degrees of freedom of a molecule on a subpicosecond time scale.[5,6] Nevertheless, in the past few years, quantum control schemes have been proposed and achieved in molecules of increasing complexity.[7−11] The aim of the present contribution is to demonstrate the coherent manipulation of atomic motion at a metal surface.

Inducing nonthermal and selective chemistry by electronic excitation of adsorbed molecules on surfaces is important in many practical applications ranging from semiconductor device fabrication to catalysis.[12,13] When a molecule is adsorbed on a metal, its photochemistry is greatly altered from the gas phase through electronic interaction with the surface. The role of the surface is 2-fold: (i) hybridization between the adsorbate and substrate orbitals results in substantially different optical absorption spectra from those of free molecules; and (ii) strong interaction with the substrate causes electronic quenching of the adsorbate typically on ≪10 fs time scale, which effectively competes with the thermalization of the electronic excitation. Thus, compared with the gas phase, molecules on surfaces can have substantially different, nonthermal chemistry, albeit with minuscule quantum yields.[12,14] A prime example is methane physisorbed on the Pt(111) surface, where thermal activation only induces desorption at 70 K, while excitation with 6.4 eV photons leads to efficient scission of the C−H bond. Since gas-phase CH_4 does not appreciably absorb light below 8.5 eV, it is remarkable that this process occurs with high selectivity and significantly lower photon energy on a metal.[15] Although the ultrafast dissipation of the electronic excitation on metals favors observation of nonthermal chemistry, it is the bane of actively manipulating surface processes by quantum control techniques.

The understanding of surface photochemistry requires direct probing of the electron−hole (e−h) pair creation and relaxation at adsorbate covered surfaces. Such studies have been greatly advanced by the development of femtosecond time-resolved two-photon photoemission (TR-2PP) techniques.[16] In analogy to multiphoton ionization techniques in the arsenal of gas-phase spectroscopy and dynamics,[6,17] TR-2PP measures the energy and momentum-resolved photoemission current following the excitation of a metal with a pump−probe laser pulse sequence. Since the two-photon excitation process can be coherent or sequential, TR-2PP experiments can distinguish between the phase relaxation of the coherent polarizations excited in the sample and the intermediate state population decay. The quasi-elastic electron−phonon (e−p) scattering mainly contributes to the phase relaxation, while the inelastic electron−electron (e−e) scattering also induces population decay. Thus, for occupied and unoccupied states that lie within several eV from the Fermi level E_F, TR-2PP can often supplant the traditional approach of estimating electronic relaxation rates from the photoemission line widths.[18]

Some of the most important findings of TR-2PP experiments are phase and energy relaxation rates of surface states. The image and crystal potentials at the surface−vacuum interface confine the surface electrons in naturally occurring quantum wells for certain ranges of energies and momenta defined by the projected band gaps in the metal band structure. Quantum confinement attenuates the surface state interaction with the bulk, resulting in decoherence times of <1−100 fs, and lifetimes in the range of <5−1000 fs.[19−23] Of particular interest are the phase relaxation times, which define the time scales for the coherent manipulation of the induced polarizations through the phase of the excitation light. Here, the optical phase is used to control the nuclear motion of Cs atoms above a Cu(111) surface.

† Part of the special issue "C. Bradley Moore Festschrift".

* Corresponding author. Current address: Department of Physics and Astronomy, University of Pittsburgh, Pittsburgh, PA 15260. E-mail: petek@pitt.edu.

10.1021/jp001218a CCC: $19.00
Published on Web 08/04/2000

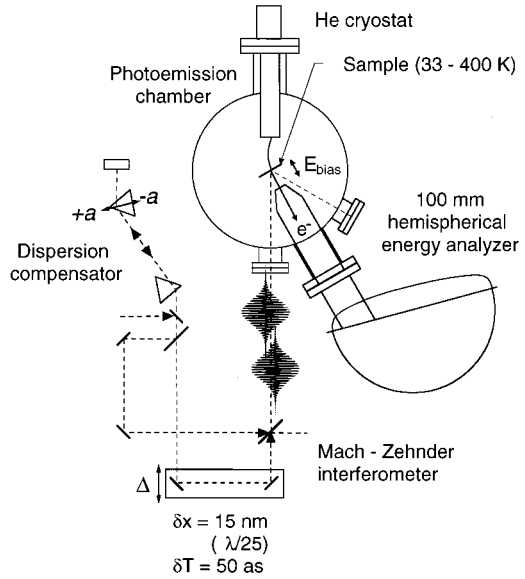

Figure 1. Schematic of the quantum control experimental apparatus. Two-photon photoemission is excited from the Cs/Cu(111) surface either with single or pulse-pair excitation, and detected with a hemispherical electron energy analyzer. The pump−probe delay Δ and chirp parameter *a* (prism insertion) are the control parameters for manipulating the coherent polarization in the sample.

II. Experimental Section

a. Experimental Apparatus. Figure 1 shows the experimental apparatus for the quantum control experiments. A more detailed description of the experiment is reported elsewhere.[16,19,24] A single-crystal sample of Cu(111) is prepared within an ultrahigh vacuum chamber by standard methods, and modified by deposition of typically 0.1 ML (1 ML (monolayer) corresponds to a Cs coverage Θ_{Cs} of 4.41×10^{14} atoms/cm^2) of Cs from a SAES getter source. The sample is held at 33 K during the TR-2PP measurements.[25−28]

Two-photon photoemission (2PP) is excited with either single pulses, or phase related pulse pairs from a self-made Ti:sapphire laser oscillator. The output of the laser is doubled to 400 nm (3.08 eV), providing an 80 MHz pulse train with an average power of ∼40 mW and pulse duration of 19 fs at the sample. The laser is incident at 30° from the normal of the sample surface and polarized in the plane of reflection (p-polarization). The normal component of the energy and momentum resolved 2PP signal is recorded with a hemispherical energy analyzer having ≤28 meV energy resolution.

Coherent polarization dynamics are probed by three different methods. Interferometric two-pulse correlation measurements are recorded for a fixed photoelectron energy by continuously scanning the pump−probe delay Δ with 50 as reproducibility by means of an actively stabilized Mach−Zender interferometer. Such measurements provide quantitative information on the phase and population decay rates,[29] as described for Cs/Cu(111) in refs 25 and 28. For quantum control experiments, 2PP spectra are recorded with either phase-locked pulse pairs (PPP), where Δ is fixed to better than 50 as, or with single frequency-chirped pulses. The linear chirp is set by the amount of glass in the optical pathway by translating one of the prisms of the dispersion compensator into or out-of the optical path.

b. Quantum Control of 2PP. Before discussing the quantum control experiments for Cs/Cu(111), it is important to introduce the band structure and previous quantum control experiments of the clean Cu(111) surface, as well as the new features that are introduced by Cs adsorption.

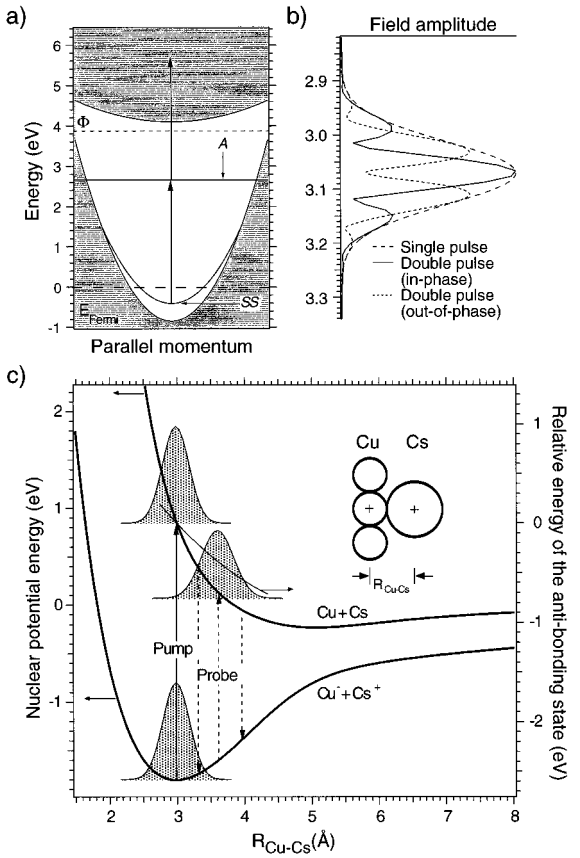

Figure 2. (a) Schematic band structure of the Cs/Cu(111) surface for parallel momentum. Unshaded area corresponds to the projected band gap. (b) Calculated electric field spectrum for a 19 fs transform-limited pulse at 3.1 eV, as well as pulse pairs of the same duration but with delays of 30.0 and 30.5 optical cycles. The interference resulting in modification of the 2PP spectra (optical Ramsey fringes) must occur in the sample, rather than the interferometer, since the pulses have negligible temporal overlap. (c) Schematic potential energy surfaces for Cs chemisorption on Cu(111),[28] and calculated change in the antibonding state energy with R_{Cu-Cs} from ref 35. Shaded curves represent the wave packet for the ground state and for dissociative motion in the excited state. The estimated change in R_{Cu-Cs} 50 fs after the excitation is 0.07 Å.[27,28] Depending on the phase of the excitation field some parts of the propagated wave packet experience constructive interference (enhanced absorption) or destructive interference (stimulated reflection), which forms the basis for quantum control. At the Cs coverage of the present experiment, $\Phi = 3.9$ eV is equal to the ionization potential of Cs atoms, and therefore, the Cs^+ and Cs products are degenerate.[28]

Figure 2a shows the schematic band structure for the Cs/Cu(111) surface as a function of parallel momentum $k_{||}$. The L-projected band gap extending from −0.85 to 4.1 eV supports a single occupied (Shockley) surface state SS with a binding energy of −0.39 eV. The photoemission line width gives a lower limit of 44 fs at 30 K for the phase relaxation time of the optically generated SS hole.[30]

Reference 24 describes the quantum control of 2PP from SS for a clean Cu(111) surface through both the PPP, or chirped pulse excitation. The following reviews these quantum control schemes. The PPP excitation exploits the optical Ramsey fringe effect, which is a coherent interaction of two separate, but phase correlated, fields acting on the sample (usually an atom or a molecule).[31] When the delay (i.e., phase) between the pump and probe fields interacting with the sample is less that the phase relaxation time of the coherent polarization in the sample, the resulting excitation spectrum depends on the relative phase. Since the transform-limited spectral width of a <20 fs excitation

pulse is broader than the homogeneous line width of SS (Γ^{SS}), the experimental line width Γ^{SS}_{exp} in single-pulse 2PP spectra is mainly determined by the laser pulse acting twice on the sample. When Δ is comparable or shorter than $(\Gamma^{SS})^{-1}$, the coherent sum of the pump- and probe-excited polarization waves in the sample will result in interference between various polarization components. Therefore, for two-pulse excitation, Γ^{SS}_{exp} is determined by Δ^{-1} rather than the transform-limited width of the individual pulses. This concept can be understood from the electric field spectra of the pulse pair when the delay is set to a $n2\pi$ multiple of the laser oscillation period at the center frequency ω_l shown in Figure 2b. Whereas the spectrum of a single pulse has a single peak, the spectra of in-phase pulse pairs have constructive interference at the center frequency and for sidebands (Ramsey fringes) at other frequencies, whenever the delay corresponds to $(n \pm 0, 1, ...)2\pi$ cycles. Likewise, destructive interference occurs for those frequency components where the delay corresponds to $(n \pm 0.5, 1.5, ...)2\pi$ cycles. Thus, spectral "squeezing" or "dilation" of the spectrum excited in the sample depends on whether or not the excitation is in-phase for the center frequency. However, Γ^{SS} sets the limit for this coherent interaction, because it represents the time scale for the memory of the phase of the excitation field in the sample.

The effect of chirp on 2PP spectra is similar, except that the phase relationship between different frequency components of a single pulse depends on the chirp parameter *a*. Since the sample has no knowledge of the entire pulse until the interaction is complete, the spectrum of the induced polarization is inversely related to the interaction time. Energy conservation requires that during the course of optical excitation an initially broad distribution must collapse through the coherent emission of the excess bandwidth, which occurs by destructive interference with the trailing part of the pulse. Since the sample has memory, the order of individual frequency components interacting with the sample can determine the final 2PP energy distribution. For instance, the leading part of a downchirped pulse (decreasing frequency with time) creates a broad excitation above the center frequency. The continuous red-shift of the instantaneous frequency causes preferentially destructive interference at high frequencies and constructive interference at low frequencies. The final spectrum is red-shifted when the rate of the frequency sweep is fast compared to the rate of phase relaxation.[24]

c. Cs Desorption. The intrinsic band structure of Cu(111) in Figure 2a is modified by the adsorption of Cs atoms. Electronic changes such as the introduction of a new unoccupied Cs antibonding state (henceforth referred to as A) and reduction in the work function Φ strongly depend on Θ_{Cs}.[32−34] Cs atoms form a disordered layer at a coverage of 0.1 ML, and therefore, the energy of A (E_A) does not disperse with $k_{||}$.[34] Since Φ determines the image potential, which in turn confines electrons to the surface, increasing Θ_{Cs} also decreases E_A, and to a smaller extent, the energy of SS. Therefore, the SS → A transition frequency can be made resonant with the laser either through a choice of Θ_{Cs} or $k_{||}$ for the 2PP detection.

A novel feature introduced by Cs adsorption is the time dependence of the surface electronic structure due to Cs atom nuclear motion.[26−28,35] Figure 2c presents the qualitative potential energy surface (PES) for chemisorption of Cs on Cu(111). This schematic is based on properties such as the ionization potential of Cs atoms, the chemisorption energy, the van der Waals potential, and the work function of the Cs/Cu(111) surface.[28] Photoexcitation induces a large redistribution of charge from the Cs−Cs bond to the vacuum side of the Cs atom,[35,36] resulting in a strong repulsion that initiates the nuclear wave packet motion. The excited state lifetime is sufficiently long (∼50 fs) to observe this motion, but too short for a significant Cs desorption yield.[27,28] Since the surface electronic structure is sensitive to the Cu−Cs bond length R_{Cu-Cs}, the wave packet motion leads to the change in the SS → A resonance frequency, which enables direct observation and control of the nuclear motion through TR-2PP techniques.[25−28,35]

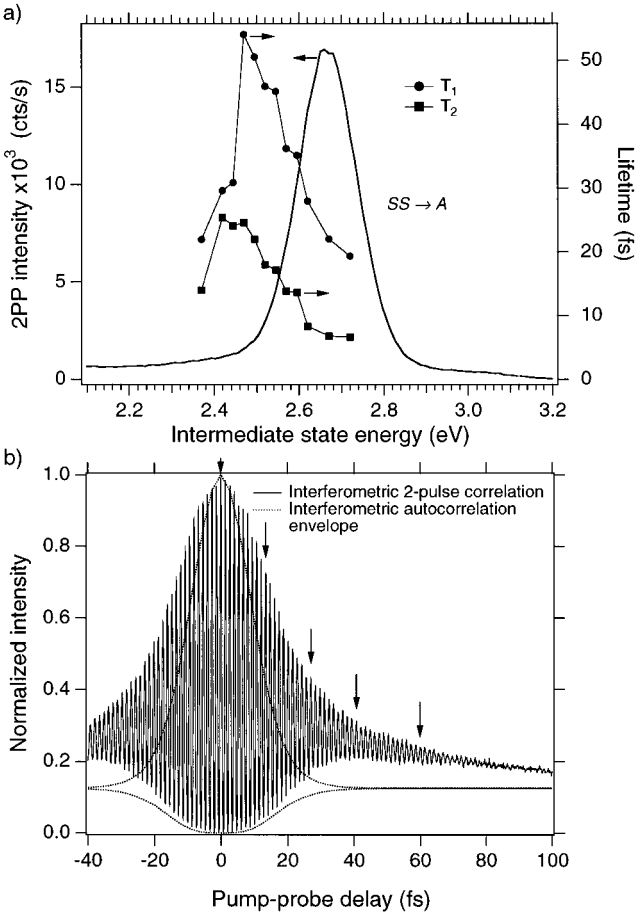

Figure 3. (a) 2PP spectrum of Cs/Cu(111) for approximately resonant SS → A excitation (∼0.1 ML Cs coverage), and the phase and energy relaxation times from interferometric two-pulse correlation scans.[25,28] (b) A representative I2PC scan measured for the intermediate state energy of 2.52 eV. The deviation of the I2PC from the envelope of the interferometric autocorrelation is due to the finite phase and energy relaxation rates. Arrows indicate the specific delay intervals of 10 cycles for the control experiments.

III. Results

Figure 3a shows a typical 2PP spectrum of the Cs/Cu(111) surface for single, minimum-chirp pulse excitation. On the basis of the band structure in Figure 2a, the peak at 2.66 eV is assigned to the one-photon resonant transition from the SS initial state at −0.42 eV to A, followed by one-photon photoemission. The assignment is confirmed by the Θ_{Cs} dependence of 2PP spectra.[26,28]

Figure 3b shows an I2PC scan taken for an intermediate state energy of 2.52 eV, i.e., ∼0.14 eV below the SS → A resonance in Figure 3a, and the envelope of the interferometric autocorrelation of the laser pulse. The I2PC scan shows rapid oscillations near $\Delta = 0$ that occur approximately at the laser frequency, and a slowly decaying component, which dominates for longer delays. Compared with the autocorrelation, the substantially broader width of the oscillatory envelope and the slow decay to the baseline of the I2PC scan indicate that the

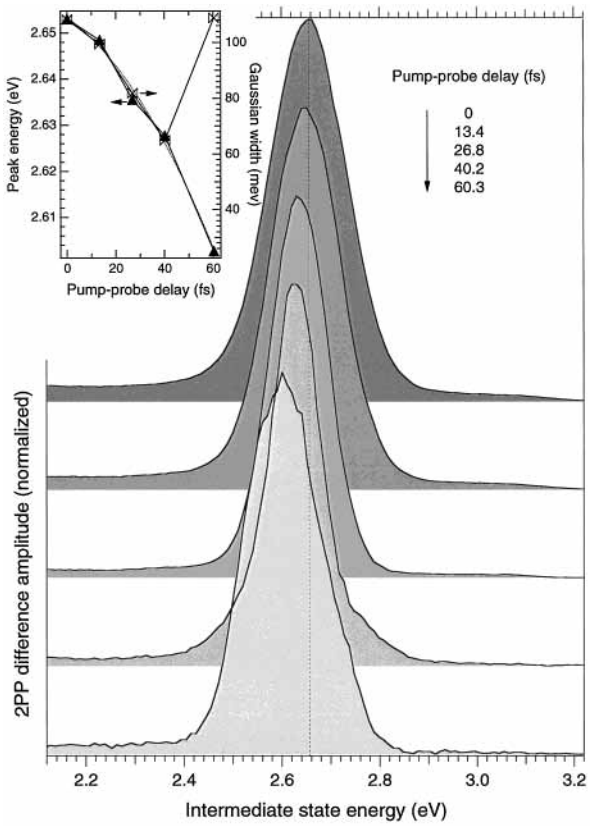

Figure 4. 2PP difference spectra for several delays corresponding to $n2\pi$ optical cycles of the center laser frequency ω_l. The vertical line represents E_A at $\Delta = 0$ fs. The inset shows the energy shift and Gaussian width of the resonance obtained by fitting the difference spectra.

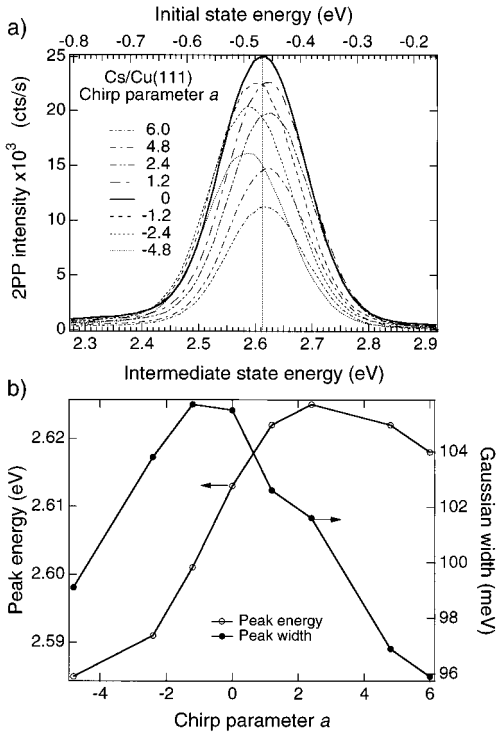

Figure 5. (a) Several 2PP spectra of the SS → A resonance for different values of the chirp parameter a. The pulse is downchirped for $a < 0$, and upchirped for $a > 0$. The dotted line indicates E_A for $a = 0$. (b) SS → A peak energy and width for different values of a.

decay of both the coherent polarization and the intermediate state population is significantly slower than the excitation pulse duration. Analysis of such I2PC scans provides the population and phase relaxation times in Figure 3a.[25,28] The focus here is on the control the Cs atom motion through the manipulation of the coherent polarization.

Since the coherent polarization decay is slower than the laser pulse, it should be possible to design specific excitation fields that can influence the position and momentum of the nuclear wave packet created through PPP and chirped pulse excitation schemes.[24]

Figure 4 shows several 2PP-difference spectra of the SS → A resonance excited with the PPP scheme. The delay between the two excitation pulses corresponds precisely to a $n2\pi$ multiple of the laser oscillation period. The difference is taken between the spectra for several delays indicated by arrows in Figure 3b and a long delay of 240 fs, where the two pulses act independently because the polarization and population relax in the intervening interval. Subtracting this background component from the short-delay spectra isolates components of the excitation process where the two pulses act jointly in a coherent or incoherent manner. As can be seen in Figure 4, the antibonding state peak in the difference spectra shifts to a lower frequency and narrows as the delay is increased. Quantitative information on the peak position and width is presented in the inset of Figure 4, which shows that both decrease with a quadratic dependence for $\Delta < 50$ fs. These changes reflect the effect of the Cs atom motion on the surface electronic structure, as well as the coherent interaction of the excitation fields in the sample.[28] While the decrease in E_A with elongation of the Cu−Cs bond is purely a response of the surface to the nuclear motion, which persists as long as the excited state population, the spectral squeezing is a consequence of electronic interference between the coherent polarizations, which decay considerably faster. After the coherence has decayed, the width reflects only the distribution of the nuclear wave packet, and hence, the width increases for $\Delta > 50$ fs.

The second approach to quantum control, where a pulse train of single, frequency-chirped pulses excites 2PP, is presented in Figure 5. The frequency chirp of the excitation pulse is determined by the total dispersion in the optical system before the sample. Linear chirp is described by the chirp parameter a, which can be calculated by the amount of fused silica inserted into or out-of the optical path. The chirp parameter a determines the rate of frequency sweep $b = \{a/(1 + a^2)\}\{1/\tau_0^2\}$, the instantaneous frequency $\omega(t) = \omega_l + bt$, the pulse width $\tau = \tau_0(1 + a^2)^{1/2}$, and the amplitude of the electric field envelope $E(a) = E_0(1 + a^2)^{-1/4}$, where τ_0 and E_0 are the width and amplitude of the unchirped pulse.[24] The condition for $a = 0$, i.e., transform-limited pulse excitation, is found by translating one of the prisms in the dispersion compensator to maximize the 2PP-count rate, which occurs for the maximum field strength, i.e. $E(0) = E_0$.

The 2PP spectra in Figure 5a show that the antibonding state peak amplitude, energy, and width depend on both the magnitude and sign of the chirp. The changes in the peak position and the width are quantified in Figure 5b by Gaussian fits of the line shapes. The peak shift and intensity are larger for downchirped pulses ($a < 0$) than for corresponding upchirped pulses. Downchirped pulses also give a broader width than the corresponding upchirped pulses. This asymmetry with regard to the sign of the chirp arises from the Cs atom dynamics.

IV. Discussion

The PPP and chirped pulse excitation schemes are essentially the same as used for the quantum control of the 2PP electron

distribution from SS for the clean Cu(111) surface;[24] however, the 2PP spectra of Cs/Cu(111) show a characteristic asymmetry, where the excitation with $\Delta > 0$ or $a < 0$ enhances the signal below the SS → A resonance that is not observed for the clean surface. The asymmetry results from the changes in the surface electronic structure due to the Cs atom nuclear wave packet dynamics, and is related to the phase and population relaxation times in Figure 3a, which peak below the SS → A resonance. The 2PP spectra are sensitive to the wave packet motion because the SS → A resonance frequency decreases as the Cu−Cs bond length R_{Cu-Cs} increases.[25,27,28,35] The simplest way to model this change is with a linear dissociative potential (constant acceleration) and a linear dependence of E_A on R_{Cu-Cs}. This directly predicts a quadratic functional form for $E_A(\Delta)$ as observed and shown in Figure 4.[27,28]

Let us now consider how the change in the SS → A resonance frequency affects the coherent dynamics. The excitation of the SS → A transition occurs at the resonance frequency of the unexcited system ω_l. After a delay Δ corresponding to $n2\pi$ optical cycles of ω_l, the resonant frequency of the excited system decreases to $\omega' = \omega_l - \Delta b$. For the same delay, the total phase in terms of ω' is $n2\pi(1 - \Delta b/\omega')$ cycles. Thus, for frequencies other than ω_l, there is in general a delay-dependent nonzero relative phase between the excitation fields. However, although the pump pulse excites a coherent polarization centered at ω_l, due to the wave packet motion, $E_A(\Delta)$ changes with Δ, and therefore the induced polarization should have a corresponding quadratic frequency chirp. Consequently, although at Δ the pump and probe fields have relative phase of Δb for ω', the evolved polarization field is in-phase with that of the probe laser at ω'.

This chirp of the induced polarization is responsible for the asymmetry in the shifts of the SS → A resonance for both the PPP and chirped-pulse excitation. In the latter case, the asymmetry arises from the fact that the dissociative wave packet motion causes a downchirp in the polarization. Since the induced polarization can maintain the in-phase relationship with the excitation field longer during the interaction with a downchirped rather than with an upchirped pulse, the 2PP signal intensity and the frequency shift are enhanced for the former.

Let us now consider what these quantum control schemes accomplish. With PPP excitation the 2PP signal from A is spectrally narrowed and shifted as a function of Δ. A narrower spectral distribution can always be achieved by exciting the sample with a single, reduced bandwidth pulse. More complex fields, such as the PPP scheme, however, are necessary to create wave packets that are both displaced from the equilibrium R_{Cu-Cs}, and narrowed in width. Likewise, the chirped pulse excitation affects the position and momentum of the wave packet, as described in a recent quantum and semiclassical simulation of the molecular Franck−Condon dynamics.[37] This can lead to effects such as wave packet focusing on ground and excited PESs, as reported for I_2.[8] Although the Cs product yield is too small to observe,[27] the manipulation of the wave packet position and momentum with the optical phase should affect the probability of desorption and the product kinetic energy distribution.

Finally, Figure 6 presents a further demonstration of quantum control with PPP excitation, which suggests how nonclassical excitation fields can manipulate atoms at surfaces. A dramatic change in the 2PP difference spectrum is observed when Δ is incremented from 30 optical cycles (40.2 fs) to 30.5 optical cycles (+0.67 fs). Whereas the consequence of in-phase excitation is a narrow displaced peak, for out-of-phase excitation it is a dip with secondary peaks below and above ω'. This occurs through the destructive interference (stimulated reflection) at ω', and constructive interference in the low- and high-energy wings. The enhancement of the low-frequency components with respect to the high-frequency components again reflects the wave packet motion. The stimulated reflection at the SS → A resonance creates a displaced wave packet on the ground PES. Thus, if the Cu−Cs desorption can be modeled with only a single coordinate R_{Cu-Cs} (i.e., ignoring phonon creation in the bulk), it should be possible to devise optical fields to drive multiple transitions between the upper and lower PES so as to enhance the dissociative motion. Furthermore, the severe limits for the quantum control of nuclear motion at metal surfaces imposed by the ultrafast electronic relaxation could be overcome by schemes such as Raman-chirped adiabatic passage,[11] which require only virtual electronic excitation. Therefore, it may be possible to manipulate with phase-modulated optical fields a variety of atomic and molecular processes such as desorption, diffusion, aggregation, alloying, as well as chemical reactions, more efficiently and with higher specificity than it is possible with single transform-limited fields.

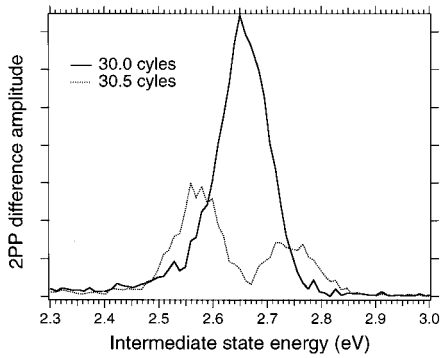

Figure 6. Two 2PP difference spectra for $\Delta = 30.0$ and 30.5 optical cycles of ω_l. The corresponding electric fields are given in Figure 2. In-phase excitation enhances the 2PP signal at the SS → A resonance and suppresses it in the wings, creating a displaced wave packet on the excited state, while out-of-phase excitation has the opposite effect, creating a displaced wave packet on the ground state.

V. Conclusions

Although, in general, quantum phase dissipation in metals is exceedingly fast, there exist a variety of bulk and surface excitations that can facilitate quantum phase control of the electronic and nuclear dynamics.[18,19,21,25,27] The example of slow phase relaxation rate for the antibonding state of Cs on Cu(111) is presently unique; however, as coherent spectroscopic techniques are increasingly applied to surfaces, further examples should emerge. Detailed studies of alkali-atom-covered metal surfaces are already helping to identify the factors that govern electronic relaxation on metal surfaces and should provide impetus to study other chemisorption and physisorption systems.[25−28,35] The present experiment demonstrates the anticipated[38,39] possibility of quantum control of atomic motion on metals. Though the challenge is high, the payoff for using coherent optical fields to manipulate atomic motion in nanoscale device fabrication, atomic scale device actuation, and molecular assembly on surfaces is potentially large.

Acknowledgment. The authors acknowledge N. Moriya, S. Matsunami, and S. Saito for technical support, J. Cina for stimulating discussions on chirped pulse excitation, and NEDO for the International Joint Research Grant, which provided partial funding for this project. M.J.W. thanks the National Science

Foundation and the Center for Global Partnership for support (NSF grant INT-9819100).

References and Notes

(1) Jasinski, J. M.; Frisoli, J. K.; Moore, C. B. *J. Chem. Soc., Faraday Trans.* **1983**, *75*, 289.
(2) Choi, Y.; Moore, C. B. *J. Chem. Phys.* **1989**, *90*, 3875.
(3) Shapiro, M.; Brumer, P. *J. Chem. Soc., Faraday Trans.* **1997**, *93*, 1263.
(4) Kawashima, H.; Wefers, M. M.; Nelson, K. A. *Annu. Rev. Phys. Chem.* **1995**, *46*, 627.
(5) Lawrance, W. D.; Moore, C. B.; Petek, H. *Science* **1985**, *227*, 895.
(6) Blanchet, V.; Zgierski, M. Z.; Seideman, T.; Stolow, A. *Nature* **1999**, *401*, 52.
(7) Zhu, L.; Kleiman, V.; Li, X.; Lu, S.; Trentelman, K.; Gordon, R. J. *Science* **1995**, *270*, 77.
(8) Kohler, B.; Yakovlev, V. V.; Che, J.; Krause, J. L.; Messina, M.; Wilson, K. R.; Schwentner, N.; Whitnell, R. M.; Yan, Y. *Phys. Rev. Lett.* **1995**, *74*, 3360.
(9) Assion, A.; Baumert, T.; Bergt, M.; Brixner, T.; Kiefer, B.; Seyfried, V.; Strehle, M.; Gerber, G. *Science* **1998**, *282*, 919.
(10) Fujimura, Y.; Gonzales, L.; Hoki, K.; Manz, J.; Otsuki, Y. *Chem. Phys. Lett.* **1999**, *306*, 1.
(11) Legare, F.; Chelkowski, S.; Bandrauk, A. D. *J. Raman Spectrosc.* **2000**, *31*, 15.
(12) *Laser Spectroscopy and Photochemistry on Metal Surfaces*; Dai, H.-L., Ho, W., Eds.; World Scientific: Singapore, 1995; Vol. 5.
(13) Ho, W. *J. Phys. Chem.* **1996**, *100*, 13050.
(14) Ho, W. *Acc. Chem. Res.* **1998**, *31*, 567.
(15) Watanabe, K.; Sawabe, K.; Matsumoto, Y. *Phys. Rev. Lett.* **1996**, *76*, 1751.
(16) Petek, H.; Ogawa, S. *Prog. Surf. Sci.* **1997**, *56*, 239.
(17) Greenblatt, B. J.; Zanni, M. T.; Neumark, D. M. *Science* **1997**, *276*, 1675.
(18) Petek, H.; Nagano, H.; Ogawa, S. *Phys. Rev. Lett.* **1999**, *83*, 832.
(19) Ogawa, S.; Nagano, H.; Petek, H.; Heberle, A. *Phys. Rev. Lett.* **1997**, *78*, 1339.
(20) Knoesel, E.; Hotzel, A.; Wolf, M. *J. Electron Spectrosc. Relat. Phenom.* **1998**, *88*−*91*, 577.
(21) Höfer, U.; Shumay, I. L.; Reuss, C.; Thomann, U.; Wallauer, W.; Fauster, T. *Science* **1997**, *277*, 1480.
(22) Purdie, D.; Hengsberger, M.; Garnier, M.; Baer, Y. *Surf. Sci.* **1998**, *407*, L671.
(23) Bartels, L.; Meyer, G.; Rieder, K.-H.; Velic, D.; Knoesel, E.; Hotzel, A.; Wolf, M.; Ertl, G. *Phys. Rev. Lett.* **1998**, *80*, 2004.
(24) Petek, H.; Heberle, A. P.; Nessler, W.; Nagano, H.; Kubota, S.; Matsunami, S.; Moriya, N.; Ogawa, S. *Phys. Rev. Lett.* **1997**, *79*, 4649.
(25) Ogawa, S.; Nagano, H.; Petek, H. *Phys. Rev. Lett.* **1999**, *82*, 1931.
(26) Petek, H.; Weida, M. J.; Nagano, H.; Ogawa, S. *Surf. Sci.* **2000**, *451*, 22.
(27) Petek, H.; Nagano, H.; Weida, M. J.; Ogawa, S. *Science* **2000**, *288*, 1402.
(28) Petek, H.; Nagano, H.; Weida, M. J.; Ogawa, S. *J. Phys. Chem.*, submitted for publication.
(29) Weida, M. J.; Ogawa, S.; Nagano, H.; Petek, H. *J. Opt. Soc. Am. B*, in press.
(30) McDougall, B. A.; Balasubramanian, T.; Jensen, E. *Phys. Rev. B* **1995**, *51*, 13891.
(31) Salour, M. M.; Cohen-Tannoudji, C. *Phys. Rev. Lett.* **1977**, *38*, 757.
(32) Fischer, N.; Schuppler, S.; Fauster, T.; Steinmann, W. *Surf. Sci.* **1994**, *314*, 89.
(33) Bauer, M.; Pawlik, S.; Aeschlimann, M. *Phys. Rev. B* **1997**, *55*, 10040.
(34) Arena, D. A.; Curti, F. G.; Bartynski, R. A. *Phys. Rev. B* **1997**, *56*, 15404.
(35) Borisov, A. G.; Kazansky, A. K.; Gauyacq, J. P. *Surf. Sci.* **1999**, *430*, 165.
(36) Ishida, H.; Liebsch, A. *Phys. Rev. B* **1992**, *45*, 6171.
(37) Shen, Y.-C.; Cina, J. A. *J. Chem. Phys.* **1999**, *110*, 9793.
(38) Plummer, W. *Science* **1997**, *227*, 1447.
(39) Wòlf, M.; Ertl, G. *Science* **2000**, *288*, 1352.